Frontiers in Bioscience Landmark

Front. Biosci. (Landmark Ed) **2026**; 31(7): 51377
https://doi.org/10.31083/FBL51377

Original Research

CRABP2 Promotes Lung Adenocarcinoma Through Retinoic Acid Pathway-Mediated NF-κB Activation

XiRui Zhu[1], BiaoFeng Fan[1], Qing Lei[1], ChenJun Xin[1], XuanCheng Li[1], ZhongRui Ma[1], SiQi Xie[1], JianLiang Shang[1], ZuYang Li[1], Chao Liu[2,*], WeiWei Wang[1,*]

[1]Department of Thoracic Surgery II, The Third Affiliated Hospital of Kunming Medical University, Yunnan Cancer Hospital, Yunnan Cancer Center, 650118 Kunming, Yunnan, China
[2]Department of Nuclear Medicine, The Third Affiliated Hospital of Kunming Medical University, Yunnan Cancer Hospital, Yunnan Cancer Center, 650118 Kunming, Yunnan, China
*Correspondence: liuchao@kmmu.edu.cn (Chao Liu); ynszlyywww@163.com (WeiWei Wang)
Academic Editor: Esteban C. Gabazza
Submitted: 1 March 2026 Revised: 22 June 2026 Accepted: 30 June 2026 Published: 27 July 2026

Abstract

Background: Lung adenocarcinoma (LUAD) is the most common subtype of non-small cell lung cancer and remains a major cause of cancer-related mortality. Despite advances in targeted therapies, tumor heterogeneity and acquired resistance frequently undermine clinical outcomes. This study aimed to identify novel oncogenic drivers and underlying mechanisms in LUAD. **Methods:** We examined cellular retinoic acid-binding protein 2 (CRABP2) expression in human LUAD specimens and evaluated its functional role through *in vitro* assays (cell proliferation, migration, invasion, and apoptosis) and *in vivo* xenograft tumor growth. Mechanistic exploration involved RNA sequencing, Kyoto Encyclopedia of Genes and Genomes (KEGG) pathway enrichment, and immunoblotting for the nuclear factor kappa B (NF-κB) signaling components, along with rescue experiments to dissect the pathway dependency. **Results:** CRABP2 was identified as a candidate oncogene in LUAD. Functional assays confirmed that CRABP2 promoted proliferation, migration, and invasion, suppressed apoptosis, and accelerated xenograft tumor growth. Mechanistically, CRABP2 potentiated retinoic acid (RA) signaling and activated the NF-κB pathway, as evidenced by enhanced inhibitor of nuclear factor kappa-B kinase subunit beta (IKKβ) phosphorylation, subsequent NF-κB inhibitor alpha (IκBα) phosphorylation, and nuclear translocation of total and phosphorylated p65. Rescue experiments revealed that CRABP2-induced NF-κB activation is RA-dependent and that this activation mediates the oncogenic effects of CRABP2. **Conclusions:** Our findings establish a CRABP2/RA/NF-κB axis that drives LUAD progression, highlighting this pathway as a potential therapeutic target for intervention in LUAD.

Keywords: retinol-binding proteins; tretinoin; NF-kappa B; adenocarcinoma of lung; cell proliferation

1. Introduction

Lung cancer remains the leading cause of cancer incidence and mortality worldwide [1]. Lung adenocarcinoma (LUAD) is one of the main histological subtypes of lung cancer [2]. Although advances in surgical resection, radiotherapy, chemotherapy, targeted therapy, and immunotherapy have improved LUAD management, patient prognosis remains poor [3]. There thus remains a pressing need to clarify the molecular mechanisms that drive LUAD and to identify novel therapeutic targets capable of guiding the more effective management of this disease.

Cellular retinoic acid-binding protein 2 (CRABP2) is a high-affinity intracellular carrier for retinoic acid (RA) [4]. It shuttles RA between the cytoplasm and the nucleus, delivering it to nuclear RA receptors (RARs) [5], thereby regulating RA-dependent transcription [6]. Aberrant CRABP2 expression has been observed in multiple cancers [7,8,9]. At a functional level, there is evidence that CRABP2 is associated with processes including differentiation, proliferation, apoptosis, and lipid metabolism [10,11,12,13]. These findings suggest that CRABP2 may serve as a prognostic marker and a potential therapeutic target.

The RA signaling pathway mediates RA-dependent control of gene expression [14]. As RA does not freely diffuse into the nucleus, the actions of carrier proteins such as CRABP2 are required for transport. In the nucleus, RA binds RAR/Retinoid X Receptor (RXR) heterodimers [15]. These heterodimers recognize retinoic acid response elements (RAREs) in target promoters and regulate transcription [15]. RA signaling tightly controls the expression of genes involved in the cell cycle, differentiation, metabolism, and apoptosis [16,17,18]. Dysregulation of the RA signaling axis has been implicated in tumorigenesis.

The nuclear factor-κB (NF-κB) pathway is a central mediator of inflammation and cancer [19,20,21]. In resting cells, NF-κB dimers (commonly p50/p65) are sequestered in the cytoplasm by inhibitor of NF-κB (IκB) proteins [22]. Extracellular stimuli such as Tumor Necrosis Factor-alpha (TNF-α), Interleukin-1 (IL-1), lipopolysaccharides (LPS), reactive oxygen species, or DNA damage activate the IκB

kinase (IKK) complex [23,24], whereupon activated IKK phosphorylates IκBα, leading to its ubiquitination and proteasomal degradation [25]. Freed NF-κB then translocates to the nucleus, binds κB motifs, and induces target gene transcription [26]. NF-κB signaling controls the expression of myriad cytokines, adhesion molecules, anti-apoptotic proteins, and cell-cycle regulators [27,28,29,30]. Persistent NF-κB activation is implicated in chronic inflammation, tumorigenesis, and metastasis [19,20,21]. While crosstalk between NF-κB signaling and other pathways has been firmly established, the interplay between RA signaling and the NF-κB axis remains to be fully characterized.

In this study, we found that CRABP2 is aberrantly overexpressed in human LUAD. We further determined that CRABP2 activates the RA signaling pathway, which, in turn, activates NF-κB signaling, ultimately promoting LUAD progression. Together, our data reveal a novel CRABP2/RA/NF-κB signaling axis while highlighting promising molecular targets as potential candidates for therapeutic intervention.

2. Materials and Methods

2.1 Gene Profiling and Sample Collection

A RNA-seq dataset consisting of normal tissue and LUAD tissue was obtained from The Cancer Genome Atlas (TCGA) database (https://portal.gdc.cancer.gov/). Paired primary tumor and adjacent non-tumorous tissues from 23 LUAD patients were obtained from the Biobank of Yunnan Provincial Cancer Hospital, with approval from the Hospital Ethics Committee. All specimens were histopathologically confirmed, staged according to the American Joint Committee on Cancer (AJCC) 9th edition Tumor, Node, Metastasis (TNM) classification system, and independently evaluated for tumor grade by two pathologists to ensure sample quality and consistency.

2.2 RNA Extraction and Sequencing Analysis of Tumor Tissues

RNA integrity was verified prior to library preparation and paired-end sequencing (150 bp) on the Illumina NovaSeq 6000 platform (NovaSeq Control Software v1.8, Illumina, Inc., San Diego, CA, USA). Following read preprocessing, alignment to the GRCh38 genome was performed using HISAT2 (v2.2.1) (Johns Hopkins University, Baltimore, MD, USA), and gene abundance was quantified with featureCounts (v2.0.1) (WEHI, Melbourne, VIC, Australia). Differentially expressed genes were identified using DESeq2 (v1.30.1) (Harvard T.H. Chan School of Public Health, Boston, MA, USA) with thresholds of $|\log2FC| > 1$ and False Discovery Rate (FDR) < 0.05.

2.3 Immunohistochemistry (IHC)

Formalin-fixed, paraffin-embedded tissue sections were deparaffinized in xylene and rehydrated through a graded ethanol series. Antigen retrieval was performed in sodium citrate buffer (pH 6.0) at 98 °C for 20 min. Endogenous peroxidase activity was blocked, and non-specific binding minimized by incubation with 5% BSA (A3858, Sigma-Aldrich, St. Louis, MO, USA) for 30 min at room temperature. Sections were incubated overnight at 4 °C with primary antibodies against CRABP2 (1:50; 10225-1-AP, Proteintech, Rosemont, IL, USA) and Ki-67 (1:50; 27309-1-AP, Proteintech, Rosemont, IL, USA). The following day, HRP-conjugated secondary antibody (ZB-2301, ZSGB-BIO, Beijing, China) was applied for 1 h at ambient temperature. Immunoreactivity was visualized using DAB, counterstained with hematoxylin, dehydrated, cleared, and mounted prior to imaging.

2.4 Cell Culture and Transfection

Human LUAD cell lines, including A549, H1299, H1650, H1734, H1975, and PC9, along with the normal bronchial epithelial line BEAS-2B and HEK-293T embryonic kidney cells, were obtained from the Cell Bank of the Chinese Academy of Sciences (Shanghai, China). A549, BEAS-2B, and HEK-293T cells were propagated in Dulbecco's modified Eagle medium (DMEM; Cytiva, Marlborough, MA, USA), whereas H1299, H1650, H1734, H1975, and PC9 cells were maintained in RPMI-1640 (Cytiva, Marlborough, MA, USA). All media were supplemented with 10% fetal bovine serum (FBS; Cytiva, Marlborough, MA, USA) and 1% penicillin-streptomycin, and cultures were maintained at 37 °C in a humidified atmosphere containing 5% CO_2. Routine testing confirmed the absence of mycoplasma contamination. All cell lines were validated by STR profiling and tested negative for mycoplasma.

CRABP2 overexpression and shRNA plasmids (Jingmai, Nanjing, China; sequences in **Supplementary Table 1**) were packaged into lentiviral particles via co-transfection with psPAX2 and pMD2.G in HEK-293T cells using Lipofectamine 3000 (Invitrogen, Carlsbad, CA, USA). Target LUAD cells were infected with viral supernatants and selected with 5 μg/mL puromycin for 7 days to establish stable overexpression or knockdown lines, which were maintained under standard culture conditions and passaged at 80% confluency.

2.5 Western Blotting

Cell lysates were prepared in RIPA buffer containing protease and phosphatase inhibitors (Leagene Biotechnology, Beijing, China) and clarified by centrifugation at 12,000 ×g for 15 min at 4 °C. Protein concentration was determined via BCA assay (Beyotime, Shanghai, China), and 20–30 μg protein per sample was resolved on 10% SDS-PAGE gels (PG112, Yamei Biotechnology, Shanghai, China) and transferred to PVDF membranes (IPVH00010, Merck KGaA, Darmstadt, Germany). Membranes were blocked with 5% nonfat milk in TBST for 1 h at ambient temperature and incubated overnight at 4 °C with primary antibodies against CRABP2 (10225-1-AP; Protein-

tech, Rosemont, IL, USA), STRA6 (22001-1-AP; Proteintech, Rosemont, IL, USA), RARβ (14013-1-AP; Proteintech, Rosemont, IL, USA), CYP26A1 (28081-1-AP; Proteintech, Rosemont, IL, USA), IKKβ (15649-1-AP; Proteintech, Rosemont, IL, USA), p-IKKβ (PR31871S; Abmart, China), IκBα (10268-1-AP; Proteintech, Rosemont, IL, USA), p-IκBα (82349-1-RR; Proteintech, Rosemont, IL, USA), p65 (10745-1-AP; Proteintech, Rosemont, IL, USA), phosphorylated p65 (p-p65) (82335-1-RR; Proteintech, Rosemont, IL, USA) and loading control antibodies against β-Actin (20536-1-AP; Proteintech, Rosemont, IL, USA), GAPDH (10494-1-AP; Proteintech, Rosemont, IL, USA), Lamin B1 (12987-1-AP; Proteintech, Rosemont, IL, USA) diluted typically 1:1000 in TBST with 5% BSA. After three TBST washes, membranes were treated with HRP-conjugated secondary antibodies (1:5000; ABclonal, Wuhan, China) for 1 h at room temperature. Signals were detected using enhanced chemiluminescence (ABclonal, Wuhan, China). For Western blot densitometry, we used ImageJ (National Institutes of Health, Bethesda, MD, USA); band intensities were normalized to loading controls (GAPDH, β-actin or Lamin B1) and expressed as fold change relative to control group.

2.6 Quantitative Real-Time Polymerase Chain Reaction (qRT-PCR)

Total RNA was isolated using TRIzol (Invitrogen, Carlsbad, CA, USA) and quantified with a NanoDrop. cDNA was synthesized from 1 μg RNA using the PrimeScript RT kit with gDNA Eraser (Takara Bio Inc., Kusatsu, Shiga, Japan). qRT-PCR was performed with SYBR Green Master Mix (Yeasen, Shanghai, China) on a real-time PCR system. Each 20 μL reaction contained 2 μL cDNA and 0.5 μM primers. Cycling: 95 °C for 10 min, 40 cycles of 95 °C for 10 s, 60 °C for 30 s. 18S rRNA served as internal control. Relative expression was calculated using the $2^{-\Delta\Delta Ct}$ method. All reactions were performed in triplicate (primer sequences in **Supplementary Table 1**).

2.7 Colony Formation Assay

For colony formation, 600 transfected cells/well were seeded in 6-well plates and cultured 10–14 days, with medium replaced every 3 days. Colonies (>50 cells) were fixed with 4% paraformaldehyde, stained with 1% crystal violet, and counted under a light microscope.

2.8 CCK-8 Cell Proliferation Assay

For short-term proliferation, 2×10^3 cells/well were plated in 96-well plates and assayed at 0, 24, 48, 72, and 96 h using CCK-8 (C0042, Beyotime, Shanghai, China), measuring absorbance at 450 nm.

2.9 EdU Incorporation Assay

EdU incorporation was performed using 10 μM EdU (C0078S, Beyotime, Shanghai, China) for 2 h, followed by fixation, permeabilization, Click-iT labeling, DAPI counterstaining, and fluorescence microscopy. At least three random fields per sample were analyzed.

2.10 Flow Cytometry Detection of Apoptosis

Apoptosis was quantified via Annexin V-FITC/PI staining (C1062S, Beyotime, Shanghai, China) and flow cytometry on an Attune NxT system (Thermo Fisher Scientific, Waltham, MA, USA). For data acquisition and analysis, cells were first gated on FSC-A vs. SSC-A to exclude debris and aggregates, followed by FSC-A vs. FSC-H to exclude doublets. Single cells were then analyzed for FITC (Annexin V) and PI fluorescence, with compensation set using single-stained controls. A minimum of 10,000 events were acquired per sample, and data were processed using CytExpert v2.0 (Beckman Coulter, Brea, CA, USA).

2.11 Wound Healing Assay

Wound healing assays were conducted by creating a scratch in confluent 6-well plates and monitoring closure over 24 h.

2.12 Transwell Migration and Invasion Assays

Transwell migration and invasion assays employed 8 μm chambers (Corning, NY, USA) with or without Matrigel coating, seeding 5×10^4–1×10^5 cells, and counting migrated/invaded cells in five random fields.

2.13 In Vivo Tumor Xenograft Assay

All experimental animals involved in this study were female BALB/c nude mice (specific pathogen-free, SPF) and were purchased from GemPharmatech Co., Ltd. (Jiangsu, China). All animals were healthy upon arrival and had no prior procedures or experimental manipulation before the start of this study. They were immunodeficient ($Foxn1^{u/N}$ genotype), lacking functional T cells, which is standard for subcutaneous xenograft models. Each animal experiment included the experimental groups and a control group, with 5 mice per group, totaling 35 mice. The experimental unit was the individual animal. The sample size (n = 5 per group) was determined based on previous similar studies on subcutaneous xenograft models. The allocation of experimental animals followed the randomization principle, using a random number table generated by [www.randomization.com] to randomly assign mice to the groups. The random sequence was generated before the start of the experiment, and each mouse was assigned a unique identification number. Based on the random sequence, animals were assigned to the control or treatment groups. The randomization was performed by an investigator not involved in the experimental procedures to ensure allocation concealment. Female BALB/c nude mice (6 weeks old) were subcutaneously injected with 5×10^5 A549 cells (CRABP2-overexpression or control) mixed 1:1 with Matrigel (354234, Corning Inc., Corning, NY, USA). Tumor

growth was monitored every 3 days, and volume calculated as (length × width^2) / 2. After 5 weeks, tumors were excised, weighed, and processed for histology. All procedures were IACUC-approved. Animals were euthanized by intraperitoneal injection of sodium pentobarbital (150 mg/kg; 50 mg/mL) at the end of the experiments. Based on the body weight of each animal (ranging from 22 g to 28 g), the injection volume was approximately 0.066–0.084 mL per animal, calculated using a pentobarbital concentration of 50 mg/mL. Specifically, for a typical animal weighing 25 g, the volume administered would be 0.075 mL, and all efforts were made to minimize suffering. This study did not involve the use of anesthetics on experimental animals, as the experimental design did not necessitate such procedures. This study was carried out in accordance with the ARRIVE guidelines.

2.14 RNA Sequencing and Transcriptomic Analysis of Cultured Cells

Total RNA from A549 cells with CRABP2 overexpression or control was isolated, and integrity verified (RIN ≥7.0). Libraries were constructed using Illumina TruSeq Stranded mRNA kit (Illumina Inc., San Diego, CA, USA) and sequenced on HiSeq X (Illumina Inc., San Diego, CA, USA) (150 bp paired-end). Reads were quality-controlled, aligned to hg38 using HISAT2, quantified with featureCounts (v2.0.1) (WEHI, Melbourne, VIC, Australia), and differential expression analyzed by DESeq2 (v1.30.1) (Harvard T.H. Chan School of Public Health, Boston, MA, USA) (adjusted $p < 0.05$). Pathway enrichment analyses were performed using standard bioinformatics tools.

2.15 Nuclear and Cytoplasmic Protein Fractionation

Nuclear and cytoplasmic proteins were separated using the Beyotime Nuclear/Cytosol Fractionation Kit (P0027, Beyotime, Shanghai, China), with fraction purity confirmed by Western blot for GAPDH and Lamin B1.

2.16 Immunofluorescence (IF)

Cells on coverslips were fixed (4% paraformaldehyde), permeabilized (0.1% Triton X-100), blocked with 5% BSA, incubated with primary (1:200) and fluorescent secondary antibodies, counterstained with DAPI, and imaged by fluorescence microscopy. The secondary antibodies used were Alexa Fluor™ 488 Goat Anti-Mouse IgG (H+L) (A-11001, Invitrogen, Waltham, MA, USA) and Alexa Fluor™ 555 Donkey Anti-Rabbit IgG (H+L) (A-31572, Invitrogen, Waltham, MA, USA).

2.17 Statistical Analysis

Data are presented as mean ± SD from at least three independent experiments. Two-group comparisons used Student's *t*-test; multi-group comparisons employed one-way ANOVA with Tukey's post hoc test. Analyses were conducted in GraphPad Prism 9.0 (San Diego, CA, USA), with significance defined as $*p < 0.05$, $**p < 0.01$, $***p < 0.001$, $****p < 0.0001$.

3. Results

3.1 CRABP2 is Significantly Overexpressed in LUAD

To identify candidate pathogenic genes in LUAD, we performed transcriptomic sequencing of three paired tumor and matched adjacent non-tumor tissue samples. CRABP2 expression was significantly upregulated in tumor tissues (Fig. 1A). Analysis of TCGA cohort corroborated this finding, with markedly higher *CRABP2* mRNA levels in LUAD as compared to matched adjacent tissues (Fig. 1B,C). We next validated these results in an independent clinical cohort, with qRT-PCR analysis of 20 paired specimens confirming significantly increased *CRABP2* mRNA levels in tumors versus matched adjacent tissues (Fig. 1D). IHC consistently confirmed stronger CRABP2 staining in tumor sections as compared with adjacent normal tissue (Fig. 1E). To investigate the prognostic significance of CRABP2 in LUAD, we analyzed multiple clinical cohorts from TCGA and Gene Expression Omnibus (GEO) databases. Survival analyses consistently demonstrated that elevated CRABP2 expression was significantly associated with poorer overall survival in patients with LUAD (Fig. 1F).

We then examined CRABP2 expression in cell lines. qRT-PCR and Western blotting analysis of six lung cancer cell lines and one normal bronchial epithelial cell line revealed CRABP2 overexpression in the cancer lines (Fig. 1G). Based on these data, A549 and PC9 cells were chosen as LUAD cell lines for use in subsequent functional studies. Stable CRABP2-overexpression and CRABP2-knockdown lines were generated via lentiviral transduction, with qRT-PCR and Western blotting confirming the expected changes in CRABP2 expression (Fig. 1H,I). Collectively, these data demonstrate that CRABP2 is overexpressed in human LUAD and provide a basis for its functional characterization in this cancer type.

3.2 CRABP2 Promotes Proliferation and Inhibits Apoptosis in LUAD Cells

In CCK-8 and colony formation assays, CRABP2 overexpression markedly enhanced the proliferation of A549 and PC9 cells, whereas CRABP2 knockdown produced the opposite effect (Fig. 2A,B). EdU incorporation assays confirmed these results, as CRABP2 overexpression raised the proportion of EdU-positive cells, whereas CRABP2 knockdown reduced EdU incorporation (Fig. 2C–E), indicating altered DNA synthesis activity. Flow cytometry revealed reciprocal effects on apoptosis, such that the rate of apoptotic death was lower among cells overexpressing CRABP2 but higher following CRABP2 knockdown (Fig. 2F,G). These data indicate an anti-apoptotic role for CRABP2. In wound healing and Transwell assays, CRABP2 overexpression enhanced the migration and invasion of A549 and PC9 cells, while CRABP2 knock-

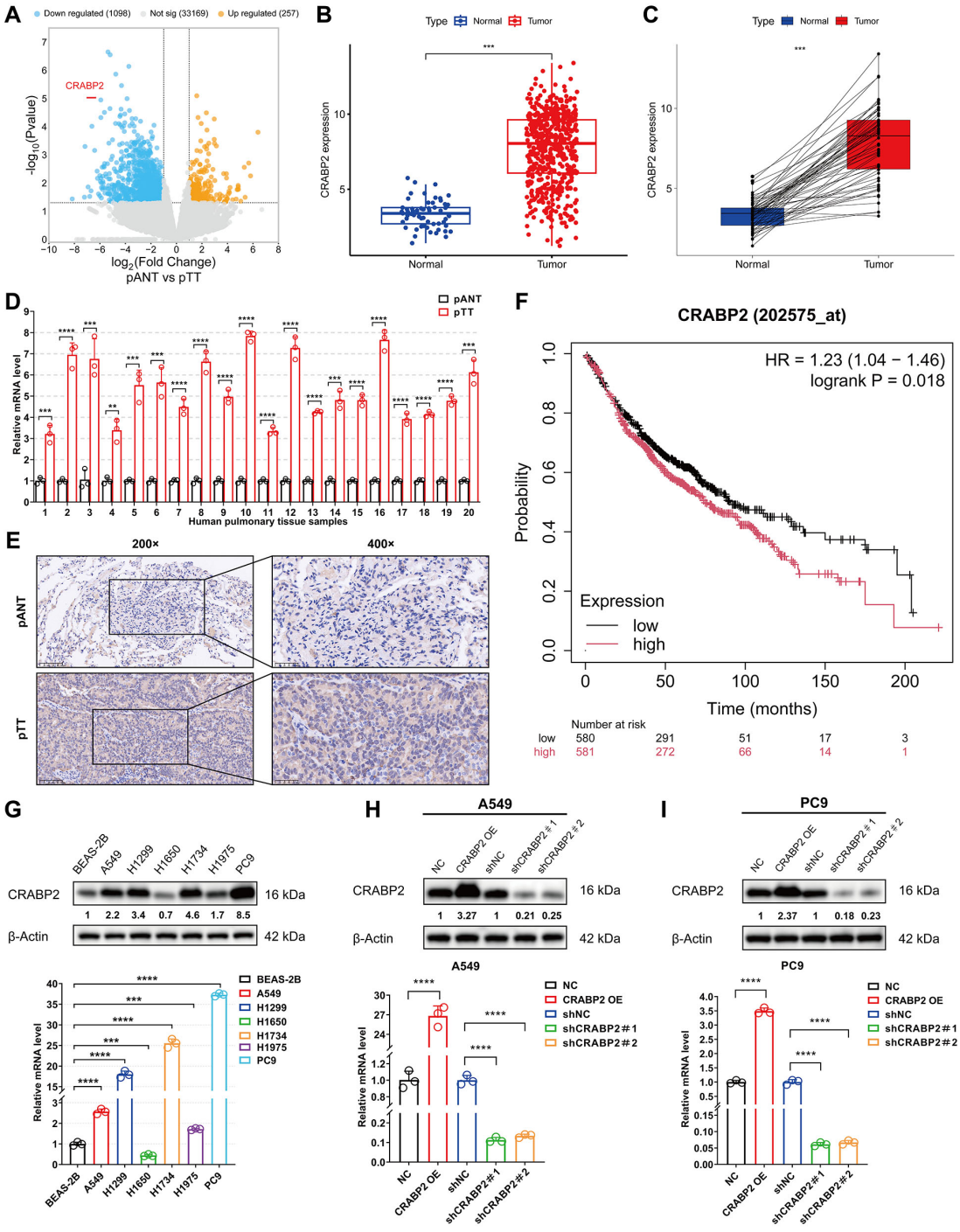

Fig. 1. Cellular retinoic acid-binding protein 2 (CRABP2) is significantly overexpressed in lung adenocarcinoma (LUAD). (A) Transcriptome (RNA-seq) analysis of three paired LUAD tumor and matched adjacent non-tumor tissues. (B,C) Analysis of The Cancer Genome Atlas (TCGA) cohort confirmed elevated *CRABP2* mRNA levels in LUAD relative to matched adjacent tissues. (D) Validation in an independent clinical cohort (n = 20 pairs) by qRT-PCR demonstrated significantly higher *CRABP2* expression in tumors. (E) Immunohistochemistry staining showed stronger CRABP2 signal in tumor tissues compared with adjacent normal sections. Scale bar, 100 μm/50 μm. (F) Kaplan-Meier survival analyses across multiple TCGA and Gene Expression Omnibus (GEO) cohorts indicated that high *CRABP2* expression was associated with poorer overall survival in LUAD patients. (G) qRT-PCR and Western blotting of six LUAD cell lines and one normal bronchial epithelial line revealed CRABP2 overexpression in cancer cells. (H,I) Stable CRABP2-overexpression and CRABP2-knockdown cell lines were established in A549 and PC9 cells via lentiviral transduction, with qRT-PCR and Western blotting confirming expected modulation of CRABP2 levels. Data are presented as mean ± SD; $^{**}p < 0.01$, $^{***}p < 0.001$, $^{****}p < 0.0001$.

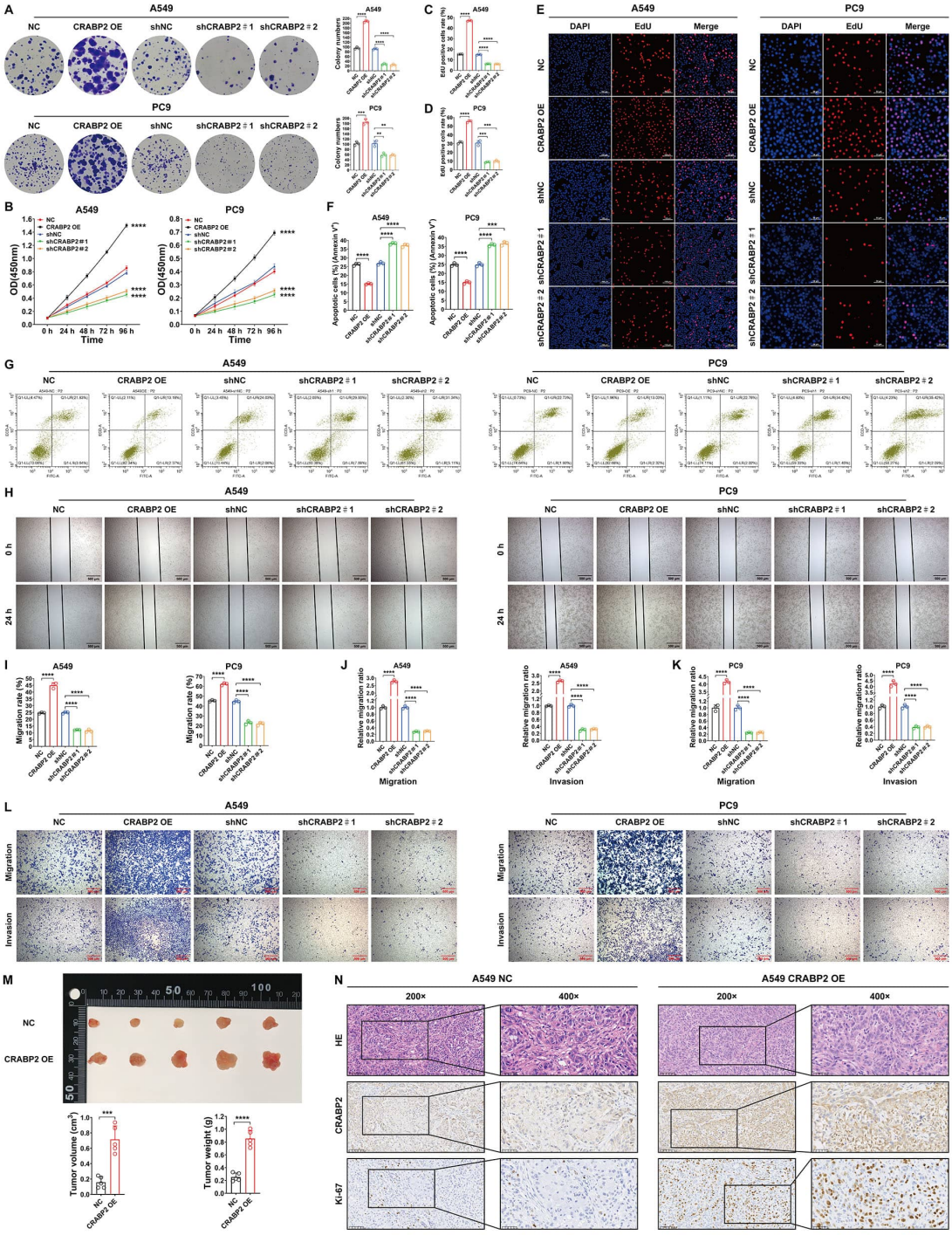

Fig. 2. Cellular retinoic acid-binding protein 2 (CRABP2) promotes proliferation and inhibits apoptosis in lung adenocarcinoma (LUAD). (A,B) Colony formation (A) and CCK-8 assays (B) show that CRABP2 overexpression (OE) increases, whereas knockdown (KD) decreases, the proliferation of A549 and PC9 cells. (C–E) EdU incorporation assay: CRABP2 OE raises the proportion of EdU-positive cells, and CRABP2 KD reduces it. Scale bar, 100 µm/50 µm. (F,G) Flow cytometric analysis reveals that CRABP2 OE reduces apoptosis, and CRABP2 KD increases apoptosis. (H–L) Wound healing and Transwell assays demonstrate that CRABP2 OE enhances migration and invasion, while CRABP2 KD impairs these abilities. Scale bars: 500 µm. (M) Subcutaneous xenograft model: mice injected with CRABP2-OE A549 cells develop larger and heavier tumors than control mice (n = 5 per group). Representative tumor images (top), quantitative analysis of tumor volume (bottom left), and quantitative analysis of tumor weight (bottom right) are shown. (N) Immunohistochemistry of Ki-67 in excised tumors shows a higher percentage of Ki-67-positive cells in the CRABP2-OE group. Scale bar, 100 µm/50 µm. All quantitative data are presented as mean ± SD; $^{**}p < 0.01$, $^{***}p < 0.001$, $^{****}p < 0.0001$.

down significantly impaired cell migration and invasion (Fig. 2H–L).

To validate these results *in vivo*, we generated subcutaneous xenografts by injecting A549 cells into nude mice. Mice injected with CRABP2-overexpressing cells developed tumors that grew faster and reached greater volumes and weights than those of control mice injected with A549-NC cells (Fig. 2M). IHC staining of excised tumors revealed a higher fraction of Ki-67 positive cells in the CRABP2-overexpression group (Fig. 2N), consistent with increased proliferative activity.

Together, these *in vitro* and *in vivo* results demonstrate that CRABP2 promotes proliferation, migration, and invasion while inhibiting apoptosis, thereby enhancing tumor growth and aggressiveness in LUAD.

3.3 CRABP2 Activates the RA Signaling Pathway

Because CRABP2 mediates RA transport and signaling, we next examined its impact on the RA pathway. In A549 and PC9 cells, qRT-PCR and Western blotting analyses showed that CRABP2 overexpression markedly increased the expression of RA target genes, including *RARB*, *STRA6*, and *CYP26A1*. In contrast, CRABP2 knockdown significantly reduced their expression (Fig. 3A,B; **Supplementary Fig. 1A**). These results demonstrate that CRABP2 overexpression activates the RA signaling pathway, whereas CRABP2 knockdown inhibits it.

3.4 CRABP2-Mediated Activation of the RA Pathway Enhances NF-κB Signaling

Previous studies have demonstrated the ability of RA signaling to regulate multiple downstream pathways, thereby exerting diverse biological effects. To examine this possibility in LUAD, we performed RNA sequencing to compare the gene expression profiles of A549 cells overexpressing CRABP2 to those of control cells. Following CRABP2 overexpression, 596 genes were significantly upregulated, while 562 genes were significantly downregulated (Fig. 3C). KEGG analysis revealed the strong enrichment of differentially expressed genes in the NF-κB signaling pathway (Fig. 3D), suggesting a potential regulatory link between CRABP2 and NF-κB signaling.

To verify this finding, we tested NF-κB activation in A549 and PC9 cells. Western blotting indicated that CRABP2 overexpression increased the phosphorylation of IKKβ (p-IKKβ) and IκBα (p-IκBα). Cytoplasmic/nuclear fractionation further revealed reduced cytoplasmic p65 and p-p65 levels, together with a corresponding increase in nuclear p65 and p-p65, indicating enhanced nuclear translocation and activation of NF-κB signaling. CRABP2 knockdown, in contrast, reduced p-IKKβ and p-IκBα levels while also increasing cytoplasmic p65 and p-p65 levels and reducing their nuclear levels (Fig. 3E–H). This suggests that CRABP2 knockdown suppresses NF-κB activation by preventing p65 and p-p65 nuclear translocation. IF staining confirmed these results, as p65 and p-p65 were predominantly localized in the nuclei of CRABP2-overexpressing cells, whereas their nuclear localization was reduced in CRABP2-knockdown cells (Fig. 3I; **Supplementary Fig. 1B**). Collectively, these results demonstrate that CRABP2 promotes NF-κB pathway activation in LUAD cells.

To test whether these effects are mediated by RA signaling, we performed rescue experiments. Treating CRABP2-overexpressing cells with the RA pathway inhibitor BMS493 for 48 h reduced p-IKKβ and p-IκBα levels. BMS493 treatment also reversed the observed nuclear accumulation of p65 and p-p65 in these cells, increasing their cytoplasmic retention. Conversely, treating CRABP2-knockdown cells with the RA agonist TTNPB for 48 h increased p-IKKβ and p-IκBα levels and promoted the nuclear translocation of p65 and p-p65 (Fig. 3J–M). IF staining yielded consistent results, demonstrating that BMS493 decreased nuclear p65/p-p65 levels, while TTNPB treatment had the opposite effect (Fig. 3N, **Supplementary Fig. 1C**).

Together, these data show that CRABP2 promotes NF-κB pathway activation by activating RA signaling in LUAD cells, and that inhibition or activation of the RA pathway can reverse the effects of CRABP2 overexpression or knockdown, respectively.

3.5 RA Signaling-Mediated Activation of the NF-κB Pathway Promotes LUAD Progression

To determine whether the tumor-promoting effects of CRABP2 are mediated via the NF-κB pathway through a mechanism regulated by RA signaling, we performed rescue experiments. Briefly, CRABP2-overexpressing A549 and PC9 cells were split into three groups and treated as follows for 48 h: Group A received the RA inhibitor BMS493; Group B received BMS493 plus the NF-κB activator LPS; and the control group received PBS. CCK-8 and colony-formation assays revealed that the proliferation of cells in Group A was markedly reduced as compared to control cells (Fig. 4A–C). EdU assays further confirmed a lower proportion of S-phase (EdU-positive) cells in Group A, indicating decreased DNA synthesis and proliferation (Fig. 4D). Flow cytometry showed increased apoptosis in Group A (Fig. 4E), while wound healing and Transwell assays revealed reduced migration and invasion in Group A (Fig. 4F–H). These data indicate that RA pathway inhibition suppresses the tumor-promoting effects of CRABP2.

Compared with Group A, Group B exhibited the restoration of malignant phenotypes. Specifically, CCK-8 and colony formation assays revealed higher proliferation in Group B (Fig. 4A–C), while EdU staining showed an increased proportion of EdU-positive cells (Fig. 4D). A reduction in apoptosis was also noted in Group B relative to Group A (Fig. 4E). Wound healing and Transwell assays also demonstrated the recovery of motility and invasive capacity in Group B (Fig. 4F–H). These results suggest that

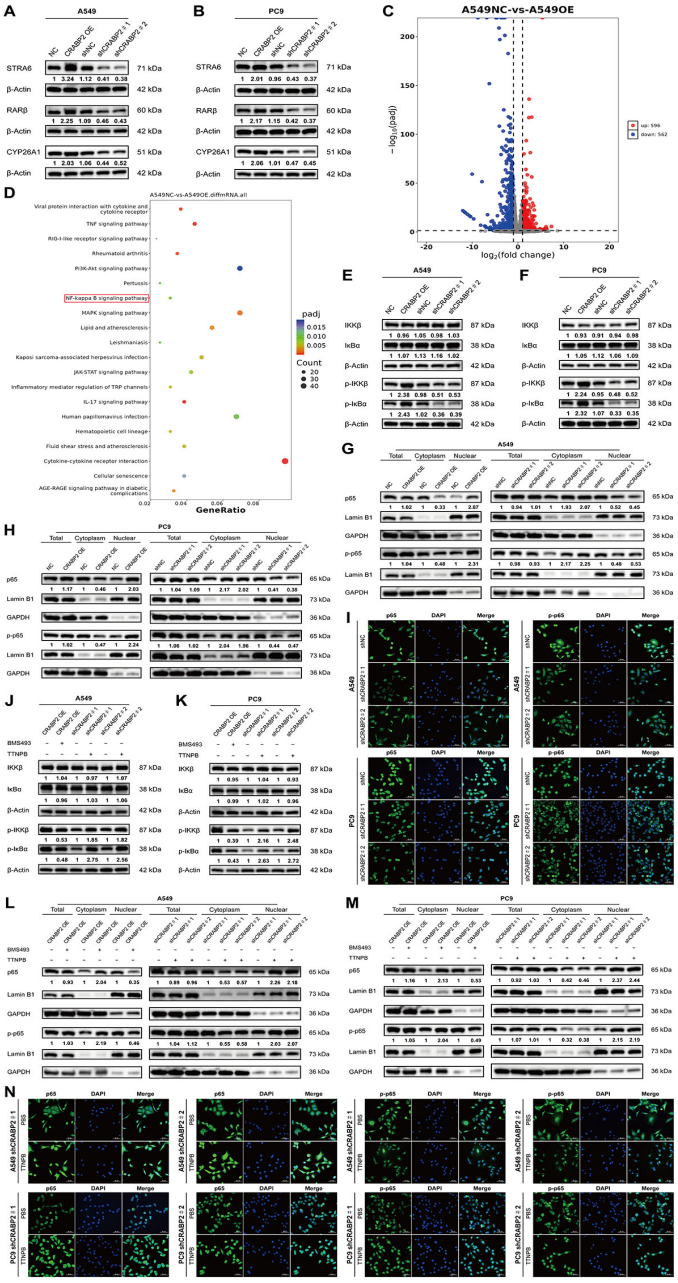

Fig. 3. Cellular retinoic acid-binding protein 2 (CRABP2)-mediated activation of the retinoic acid (RA) pathway enhances the nuclear factor kappa B (NF-κB) signaling. (A,B) Western blot analyses of RA target genes (*RARB*, *STRA6*, *CYP26A1*) in A549 and PC9 cells. CRABP2 overexpression (OE) markedly increases their expression, whereas CRABP2 knockdown (KD) significantly reduces it. (C) Volcano plot of RNA-seq analysis showing differentially expressed genes following CRABP2 overexpression in A549 cells (596 upregulated, 562 downregulated). (D) Kyoto Encyclopedia of Genes and Genomes (KEGG) pathway enrichment analysis highlighting NF-κB signaling as significantly enriched. (E–H) Western blot analysis (E,F) and cytoplasmic/nuclear fractionation (G,H) in A549 and PC9 cells. CRABP2 OE increases phosphorylation of inhibitor of nuclear factor kappa-B kinase subunit beta (IKKβ) and NF-κB inhibitor alpha (IκBα), reduces cytoplasmic p65/phosphorylated p65 (p-p65), and increases nuclear p65/p-p65; CRABP2 knockdown (KD) produces opposite effects. (I) Immunofluorescence staining of p65 and p-p65 in A549 cells. CRABP2 OE promotes nuclear localization, whereas CRABP2 KD reduces it. Scale bar, 50 μm. See also **Supplementary Fig. 1B**. (J–M) Rescue experiments with the RA pathway inhibitor BMS493 (in CRABP2-OE cells) and the RA agonist TTNPB (in CRABP2-KD cells). BMS493 reduces phosphorylated IKKβ (p-IKKβ)/phosphorylated IκBα (p-IκBα) and reverses nuclear accumulation of p65/p-p65; TTNPB increases these phosphorylation events and promotes nuclear translocation. (N) Immunofluorescence staining confirming that BMS493 decreases nuclear p65/p-p65, while TTNPB increases it. Scale bar, 50 μm. See also **Supplementary Fig. 1C**. The concentrations, administration methods, and treatment durations of all reagents and pharmacological agents are provided in **Supplementary Table 2**.

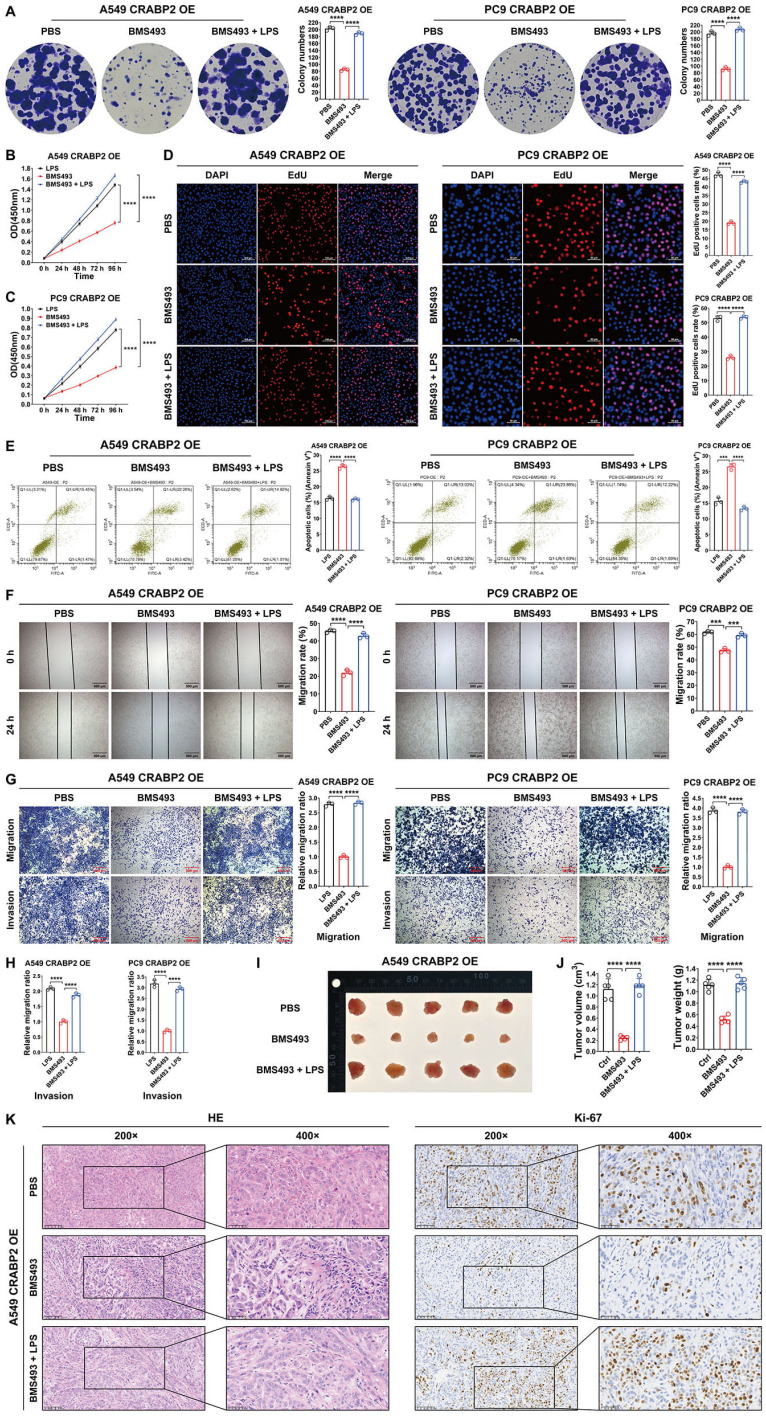

Fig. 4. Retinoic acid (RA) signaling-mediated activation of the nuclear factor kappa B (NF-κB) pathway promotes lung adenocarcinoma (LUAD) progression. (A–C) Colony formation (A) and CCK-8 assays (B,C) in CRABP2-overexpressing A549 and PC9 cells. Group A (RA inhibitor BMS493) shows reduced proliferation versus control; Group B (BMS493 + NF-κB activator LPS) restores proliferation relative to Group A. (D) EdU incorporation assay. Group A has fewer EdU-positive cells (decreased DNA synthesis), while Group B reverses this effect. Scale bar, 100 μm/50 μm. (E) Flow cytometry analysis of apoptosis. Group A shows increased apoptosis; Group B shows reduced apoptosis relative to Group A. (F–H) Wound healing (F) and Transwell migration/invasion (G,H) assays. Group A exhibits impaired migration and invasion, which are restored in Group B. Scale bars: 500 μm. (I–K) Subcutaneous xenograft model in nude mice (n = 5 per group). Group A (BMS493) shows slower tumor growth, smaller volume and weight, and fewer Ki-67-positive cells; Group B (BMS493 + LPS) restores tumor growth and proliferation to near-control levels. Scale bar, 100 μm/50 μm. All quantitative data are presented as mean ± SD; ***$p < 0.001$, ****$p < 0.0001$. The concentrations, administration methods, and treatment durations of all reagents and pharmacological agents are provided in **Supplementary Table 2**.

NF-κB activation can rescue the tumor-suppressing effect imposed by RA blockade. Thus, the tumor-promoting effects of CRABP2 require RA signaling and are, at least partially, mediated via NF-κB activation.

To expand on these findings *in vivo*, we generated subcutaneous xenografts by injecting CRABP2-overexpressing A549 cells into nude mice. Mice were then assigned to three groups and treated daily for 5 weeks as follows: Group A received BMS493 (RA inhibitor), Group B received BMS493 plus LPS (NF-κB activator), and the control group received PBS. After 5 weeks, mice were sacrificed and tumors were collected. Tumors in Group A grew more slowly than those in control mice (Fig. 4I), and both tumor volume and tumor weight were significantly smaller in Group A (Fig. 4J). IHC revealed a smaller fraction of Ki-67-positive cells in tumors from Group A, indicating reduced proliferative activity (Fig. 4K). These findings demonstrate that RA pathway inhibition suppresses the tumor-promoting effects of CRABP2. In Group B, tumor growth was faster than in Group A (Fig. 4I), with tumor volumes and weights that were significantly larger than those in Group A, approaching the levels observed in controls (Fig. 4J). Ki-67 staining revealed a higher proportion of proliferating cells in Group B (Fig. 4K). These data show that NF-κB activation can restore the CRABP2-driven tumor growth suppressed by RA blockade.

Together with our *in vitro* results, these *in vivo* data support the ability of CRABP2 to promote tumor growth via the RA signaling-dependent activation of the NF-κB signaling pathway.

3.6 Inhibition of NF-κB Signaling Suppresses CRABP2-Mediated Tumor-Promoting Effects

To further investigate the role of NF-κB in CRABP2-driven tumor growth, we performed rescue experiments. Briefly, CRABP2-overexpressing A549 and PC9 cells were treated with the NF-κB inhibitor BAY11-7082 for 48 h. CCK-8 and colony formation assays revealed a marked reduction in cell proliferation in response to NF-κB inhibition (Fig. 5A–D). EdU assays confirmed that such treatment was associated with the presence of fewer EdU-positive cells, indicating decreased DNA synthesis (Fig. 5E,F). Flow cytometry revealed a significant increase in apoptosis (Fig. 5G,H). Wound-healing and Transwell assays showed reduced migration and invasion (Fig. 5I–M). These results indicate that NF-κB inhibition suppresses the tumor-promoting effects of CRABP2 *in vitro*.

To further determine whether RA signaling functions upstream of NF-κB activation, CRABP2-overexpressing A549 and PC9 cells were co-treated with BAY11-7082 and the RAR agonist TTNPB for 48 h. Compared with BAY11-7082 treatment alone, co-treatment with TTNPB significantly restored cell proliferation, as demonstrated by CCK-8 and colony formation assays (Fig. 5A–D). Similarly, EdU assays showed a marked increase in the proportion of EdU-positive cells in the BAY11-7082 + TTNPB group, indicating enhanced DNA synthesis (Fig. 5E,F). Flow cytometric analysis further revealed that TTNPB treatment significantly reduced the apoptotic rate induced by BAY11-7082 (Fig. 5G,H). In addition, wound healing and Transwell assays demonstrated partial recovery of migratory and invasive abilities following TTNPB treatment (Fig. 5I–M). These results indicate that activation of RA signaling can reverse the tumor-suppressive effects caused by NF-κB inhibition. Taken together, these findings further support a model in which RA signaling acts upstream of NF-κB signaling and promotes CRABP2-mediated malignant progression in LUAD.

For *in vivo* validation, we established subcutaneous xenografts by injecting A549 cells overexpressing CRABP2 into nude mice. The treatment group received intraperitoneal BAY11-7082 daily, while controls received equal volumes of PBS. After five weeks, mice were sacrificed and tumors were collected. Tumors from the BAY11-7082-treated group grew more slowly than those from controls (Fig. 5N). Both tumor volume and tumor weight were significantly reduced in the treated group (Fig. 5N). IHC staining revealed a lower fraction of Ki-67-positive cells in treated tumors, indicating a reduction in proliferative activity (Fig. 5O).

Collectively, these *in vitro* and *in vivo* results show that NF-κB inhibition suppresses the tumor-promoting effects of CRABP2, consistent with CRABP2 acting through NF-κB activation to drive LUAD progression.

4. Discussion

RA and its associated signaling pathways play multifaceted roles in tumor biology. Clinical and molecular epidemiological studies have shown that aberrant regulation of RA signaling is common in many solid tumors, including non-small cell lung cancer (NSCLC) [31,32,33]. In NSCLC, hypermethylation of CpG islands in the *RARB* promoter frequently leads to gene silencing [34]. This suggests that epigenetic inactivation of *RARB* is a key mechanism contributing to tumor initiation and progression. Beyond receptor-level regulation, intracellular components of the RA pathway are also dysregulated in the context of oncogenic activity. For example, the RA-binding protein CRABP2 is abnormally expressed in lung cancer [35]. Its high expression correlates with increased invasion, metastasis, and poor prognosis. This suggests that, in addition to nuclear receptors, RA signaling is controlled by intracellular transport, binding proteins, and metabolic enzymes, which together shape tumor cell behavior at the molecular level [36,37,38]. These observations have prompted extensive interest in RA and its analogs, such as all-trans RA (ATRA), in cancer prevention and treatment [39]. Early clinical trials explored the single-agent utility of ATRA, while preclinical research examined its synergistic effects when combined with chemotherapy or immunother-

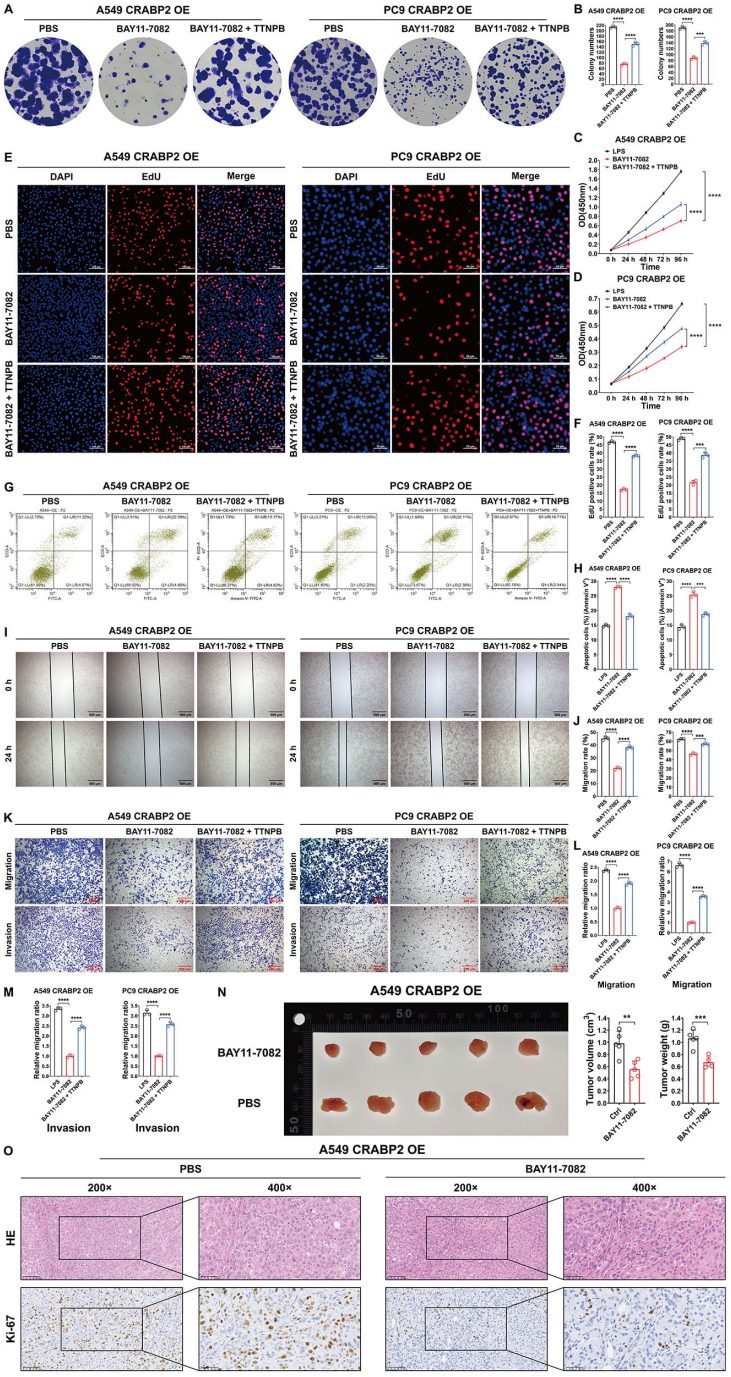

Fig. 5. Inhibition of nuclear factor kappa B (NF-κB) signaling suppresses cellular retinoic acid-binding protein 2 (CRABP2)-mediated tumor-promoting effects. (A–D) Colony formation (A,B) and CCK-8 assays (C,D) in CRABP2-overexpressing A549 and PC9 cells. BAY11-7082 (NF-κB inhibitor) reduces proliferation; co-treatment with TTNPB (RAR agonist) restores proliferation. (E,F) EdU incorporation assay. BAY11-7082 decreases EdU-positive cells (reduced DNA synthesis), and TTNPB reverses this effect. Scale bar, 100 μm/50 μm. (G,H) Flow cytometry analysis of apoptosis. BAY11-7082 increases apoptosis; TTNPB reduces apoptosis induced by BAY11-7082. (I–M) Wound healing (I,J) and Transwell migration/invasion assays (K–M). BAY11-7082 impairs migration and invasion; TTNPB partially restores these capacities. Scale bars: 500 μm. (N) Subcutaneous xenograft model in nude mice (n = 5 per group). Daily intraperitoneal BAY11-7082 significantly reduces tumor growth, volume, and weight compared with control (PBS). (O) Immunohistochemistry of Ki-67 in excised tumors. BAY11-7082 treatment decreases the fraction of Ki-67-positive cells, indicating reduced proliferation. Scale bar, 100 μm/50 μm. All quantitative data are presented as mean ± SD; $^{**}p < 0.01$, $^{***}p < 0.001$, $^{****}p < 0.0001$. The concentrations, administration methods, and treatment durations of all reagents and pharmacological agents are provided in **Supplementary Table 2**.

apy [40]. Collectively, these studies highlight the importance of the RA pathway as both a key regulator of lung cancer biology and a promising therapeutic target. Further research focused on the RA pathway centered on epigenetic regulation, signaling crosstalk, and combination treatment strategies may provide new opportunities for precision therapy in lung cancer.

Importantly, the RA signaling pathway not only directly regulates target gene expression but also interacts with multiple signaling cascades to influence tumor progression. Studies have shown that RA signaling modulates key oncogenic pathways, including the MAPK, PI3K/Akt, Wnt/β-catenin, and TGF-β pathways [41,42,43]. For example, activation of the RA-RARα signaling axis induces ERK1/2 phosphorylation and enhances tumor cell migration [33]. The RA-RXR complex interacts with β-catenin, altering the transcription of Wnt target genes [44]. In addition, RA-mediated cooperation with Smad signaling plays a critical role in epithelial-mesenchymal transition (EMT) regulation [45]. Together, these findings suggest that abnormal RA signaling drives intrinsic tumor cell behavior while also reshaping the tumor microenvironment and promoting immune evasion.

In LUAD, the relationship between RA signaling and NF-κB signaling has not been well established. Here, we found that CRABP2 markedly activates RA signaling. Because CRABP2 functions mainly as a carrier and transporter of RA, its overexpression may increase nuclear RA availability, thus enhancing RAR-mediated transcription. Transcriptomic sequencing of CRABP2-overexpressing A549 cells revealed 596 upregulated and 562 downregulated genes relative to control cells. KEGG pathway analysis showed significant enrichment in the NF-κB signaling pathway, suggesting that CRABP2 may influence NF-κB activation through RA signaling. To verify this hypothesis, we examined NF-κB pathway components via Western blotting and IF staining, ultimately confirming that CRABP2 regulates NF-κB pathway activity. Moreover, in rescue experiments, the effects of CRABP2 overexpression or knockdown on NF-κB signaling were reversed by RA pathway inhibition or activation, respectively. These findings demonstrate that CRABP2 regulates the NF-κB signaling pathway via RA signaling, uncovering a new molecular link between these two pathways in the development of LUAD.

Extensive evidence shows that the NF-κB signaling pathway plays a central role in tumor initiation and progression. At the molecular level, NF-κB drives expression of pro-survival and proliferative genes, pro-inflammatory cytokines, and angiogenic factors [46,47,48]. These changes give tumor cells anti-apoptotic advantages, facilitate metabolic reprogramming, and provide vascular support. NF-κB also promotes EMT activity and metastasis by inducing the expression of matrix metalloproteinases, chemokine receptors, and EMT-associated transcription factors across multiple solid tumors [49,50,51]. Persistent NF-κB activation also increases resistance to chemotherapy and radiotherapy, contributing to therapeutic failure [52,53].

Many studies have reported aberrant NF-κB activation in NSCLC. Increased NF-κB expression or activity correlates with disease progression and poorer overall survival [54,55,56]. Mechanistic research has further demonstrated that NF-κB inhibition in p53-deficient mice induces apoptosis and slows LUAD growth, while galectin-3 activates Toll-like receptor 4 (TLR4)-NF-κB signaling to increase NEAT1, driving proliferation and migration, and MYC-associated zinc finger protein (MAZ) activates NF-κB to promote tumor growth and immune evasion [57,58,59]. These data underscore the promise of NF-κB as a promising therapeutic target. Preclinical and early clinical studies suggest that combining NF-κB inhibitors with chemotherapy or immunotherapy can enhance efficacy and help overcome therapeutic resistance [60,61].

In our study, CRABP2 promoted proliferation and suppressed apoptosis in LUAD cells. Blocking the RA signaling pathway markedly weakened this effect, indicating that the tumor-promoting effects of CRABP2 depend on RA signaling. Activating NF-κB restored the ability of CRABP2 to promote tumor development even when RA signaling was inhibited. Conversely, NF-κB inhibition strongly attenuated the tumor-promoting effects of CRABP2. Together, these results indicate that CRABP2 drives tumor progression by activating NF-κB, and that NF-κB activation is contingent on CRABP2-mediated RA pathway activation.

In conclusion, our study shows that CRABP2 is significantly upregulated in LUAD and actively promotes tumor progression, identifying the CRABP2/RA signaling/NF-κB pathway axis as a novel mechanism underlying this effect. These findings expand mechanistic understanding of CRABP2 in LUAD and suggest that CRABP2 and its downstream pathways may offer utility as candidate diagnostic, prognostic, and therapeutic targets.

5. Limitations

Despite the significant findings presented in this study, several limitations should be acknowledged. First, while our transcriptome sequencing and validation cohorts consistently demonstrated CRABP2 upregulation in LUAD, the sample size for the in-house validation (20 paired specimens for qRT-PCR and three paired samples for sequencing) was relatively modest. Larger, multicenter clinical cohorts with long-term follow-up data are needed to definitively establish the clinical and prognostic value of CRABP2 expression. Second, although we demonstrate that CRABP2 activates RA signaling and subsequently the NF-κB pathway, the precise molecular interactions require further mechanistic dissection, including co-immunoprecipitation and chromatin immunoprecipitation (ChIP) assays. Third, our *in vivo* experiments relied solely

on subcutaneous xenograft models using A549 cells. While informative, these models do not fully recapitulate the native tumor microenvironment, immune interactions (as they were performed in nude mice), or the metastatic process. Future studies using orthotopic mouse models, immunocompetent models, or patient-derived xenografts (PDXs) would provide more clinically relevant insights. Fourth, although CRABP2 is known to facilitate nuclear delivery of RA and activation of RAR-dependent transcription, direct assessment of RA nuclear trafficking and CRABP2–RAR interactions in LUAD cells was not performed in the present study and warrants further investigation. Finally, the potential functional redundancy between CRABP2 and other RA-binding proteins, such as cellular retinoic acid-binding protein 1 (CRABP1) or fatty acid-binding protein 5 (FABP5), was not explored. It remains possible that these related proteins may compensate for or interact with CRABP2, particularly in resistant cell lines.

6. Conclusion

In summary, this study identifies CRABP2 as a significantly overexpressed oncogene in LUAD that drives malignant progression. We demonstrate that CRABP2 exerts its tumor-promoting effects—enhanced proliferation, migration, invasion, and reduced apoptosis—by activating a novel CRABP2/RA signaling/NF-κB signaling axis. Mechanistically, CRABP2 upregulation activates the RA signaling pathway, which in turn promotes IKKβ/IκBα phosphorylation and nuclear translocation of p65/p-p65, thereby triggering NF-κB activation. Rescue experiments confirmed that the functional consequences of CRABP2 are dependent on this sequential pathway activation, as pharmacological inhibition of either RA or NF-κB signaling abrogated CRABP2-driven malignancy, while activation of NF-κB restored it. Collectively, these findings not only expand our understanding of CRABP2 biology in LUAD but also provide a strong preclinical rationale for targeting the CRABP2/RA/NF-κB axis as a potential therapeutic strategy for LUAD. Moreover, CRABP2 and its downstream effectors may serve as valuable diagnostic biomarkers or predictive indicators of response to therapies targeting these pathways.

Availability of Data and Materials

The datasets generated and analyzed during the current study are available from the corresponding authors upon reasonable request.

Author Contributions

Conceptualization: XRZ, WWW; Statistical analysis: BFF, ZRM; Methodology: QL, CL, ZRM; Formal analysis: CJX, ZYL; Data acquisition and manuscript writing: XRZ, XCL; Investigation and data curation: ZRM, SQX; Conception and design: JLS, WWW. All authors have read and agreed to the published version of the manuscript. All authors contributed to editorial changes in the manuscript. All authors have participated sufficiently in the work and agreed to be accountable for all aspects of the work.

Ethics Approval and Consent to Participate

This study was approved by the Ethics Committee of [Kunming Medical University] (Approval No. KMMU20230710) and conducted in compliance with the Guide for the Care and Use of Laboratory Animals published by the US National Institutes of Health (NIH Publication No. 85-23, revised 1996). All efforts were made to minimize animal suffering and to reduce the number of animals used. This study was carried out in accordance with the ARRIVE guidelines. All human tissues involved in this study were obtained from the Biobank of Yunnan Cancer Hospital and were approved by the Ethics Committee of [Yunnan Cancer Hospital] (Approval No. KYLX2025-305). Informed consent was obtained from all participants prior to sample collection and storage in the Biobank of Yunnan Cancer Hospital. The study was carried out in accordance with the guidelines of the Declaration of Helsinki.

Acknowledgment

Not applicable.

Funding

This work was supported by Key Clinical Research Project of the “Kunyi Leading Research” Program of Kunming Medical University (NO. QL-JBGS-02), Joint Program of Applied Basic Research of Yunnan Provincial Department of Science and Technology - Kunming Medical University (NO. 202301AY070001-106), and Key Project of the Joint Special Program of Kunming Medical University (NO. 202401AB070049).

Conflicts of Interest

The authors declare that the research was conducted in the absence of any commercial or financial relationships that could be construed as a potential conflict of interest.

Supplementary Material

Supplementary material associated with this article can be found, in the online version, at https://doi.org/10.31083/FBL51377.

References

[1] Bray F, Laversanne M, Sung H, Ferlay J, Siegel RL, Soerjomataram I, et al. Global cancer statistics 2022: GLOBOCAN estimates of incidence and mortality worldwide for 36 cancers in 185 countries. CA: a Cancer Journal for Clinicians. 2024; 74: 229–263. https://doi.org/10.3322/caac.21834

[2] Zhang Y, Vaccarella S, Morgan E, Li M, Etxeberria J, Chokunonga E, et al. Global variations in lung cancer incidence by histological subtype in 2020: a population-based study.

The Lancet. Oncology. 2023; 24: 1206–1218. https://doi.org/10.1016/S1470-2045(23)00444-8
[3] Belaroussi Y, Bouteiller F, Bellera C, Pasquier D, Perol M, Debieuvre D, et al. Survival outcomes of patients with metastatic non-small cell lung cancer receiving chemotherapy or immunotherapy as first-line in a real-life setting. Scientific Reports. 2023; 13: 9584. https://doi.org/10.1038/s41598-023-36623-1
[4] Yabut KCB, Isoherranen N. CRABPs Alter *all-trans*-Retinoic Acid Metabolism by CYP26A1 via Protein-Protein Interactions. Nutrients. 2022; 14: 1784. https://doi.org/10.3390/nu14091784
[5] Dong D, Ruuska SE, Levinthal DJ, Noy N. Distinct roles for cellular retinoic acid-binding proteins I and II in regulating signaling by retinoic acid. The Journal of Biological Chemistry. 1999; 274: 23695–23698. https://doi.org/10.1074/jbc.274.34.23695
[6] Delva L, Bastie JN, Rochette-Egly C, Kraïba R, Balitrand N, Despouy G, et al. Physical and functional interactions between cellular retinoic acid binding protein II and the retinoic acid-dependent nuclear complex. Molecular and Cellular Biology. 1999; 19: 7158–7167. https://doi.org/10.1128/MCB.19.10.7158
[7] Jin BY, Fu GH, Jiang X, Pan H, Zhou DK, Wei XY, et al. CRABP2 and FABP5 identified by 2D DIGE profiling are up-regulated in human bladder cancer. Chinese Medical Journal. 2013; 126: 3787–3789.
[8] Toyama A, Suzuki A, Shimada T, Aoki C, Aoki Y, Umino Y, et al. Proteomic characterization of ovarian cancers identifying annexin-A4, phosphoserine aminotransferase, cellular retinoic acid-binding protein 2, and serpin B5 as histology-specific biomarkers. Cancer Science. 2012; 103: 747–755. https://doi.org/10.1111/j.1349-7006.2012.02224.x
[9] Liu RZ, Li S, Garcia E, Glubrecht DD, Poon HY, Easaw JC, et al. Association between cytoplasmic CRABP2, altered retinoic acid signaling, and poor prognosis in glioblastoma. Glia. 2016; 64: 963–976. https://doi.org/10.1002/glia.22976
[10] Yuan J, Tang Z, Yang S, Li K. CRABP2 promotes myoblast differentiation and is modulated by the transcription factors MyoD and Sp1 in C2C12 cells. PloS One. 2013; 8: e55479. https://doi.org/10.1371/journal.pone.0055479
[11] Vo HP, Crowe DL. Transcriptional regulation of retinoic acid responsive genes by cellular retinoic acid binding protein-II modulates RA mediated tumor cell proliferation and invasion. Anticancer Research. 1998; 18: 217–224.
[12] Vreeland AC, Levi L, Zhang W, Berry DC, Noy N. Cellular retinoic acid-binding protein 2 inhibits tumor growth by two distinct mechanisms. The Journal of Biological Chemistry. 2014; 289: 34065–34073. https://doi.org/10.1074/jbc.M114.604041
[13] Xia J, Peng B, Wang J, Li F, Long G. CRABP2 promotes metastasis and lipid droplet accumulation in non-small cell lung cancer by downregulating PLAAT4. Journal of Cancer. 2025; 16: 2917–2928. https://doi.org/10.7150/jca.112019
[14] Panariello L, Quadro L, Trematerra S, Colantuoni V. Identification of a novel retinoic acid response element in the promoter region of the retinol-binding protein gene. The Journal of Biological Chemistry. 1996; 271: 25524–25532. https://doi.org/10.1074/jbc.271.41.25524
[15] Xiao JH, Durand B, Chambon P, Voorhees JJ. Endogenous retinoic acid receptor (RAR)-retinoid X receptor (RXR) heterodimers are the major functional forms regulating retinoid-responsive elements in adult human keratinocytes. Binding of ligands to RAR only is sufficient for RAR-RXR heterodimers to confer ligand-dependent activation of hRAR beta 2/RARE (DR5). The Journal of Biological Chemistry. 1995; 270: 3001–3011. https://doi.org/10.1074/jbc.270.7.3001
[16] Chen Q, Ross AC. Retinoic acid regulates cell cycle progression and cell differentiation in human monocytic THP-1 cells. Experimental Cell Research. 2004; 297: 68–81. https://doi.org/10.1016/j.yexcr.2004.02.017
[17] Mamoon A, Subauste A, Subauste MC, Subauste J. Retinoic acid regulates several genes in bile acid and lipid metabolism via upregulation of small heterodimer partner in hepatocytes. Gene. 2014; 550: 165–170. https://doi.org/10.1016/j.gene.2014.07.017
[18] Heo SH, Kwak J, Jang KL. All-trans retinoic acid induces p53-depenent apoptosis in human hepatocytes by activating p14 expression via promoter hypomethylation. Cancer Letters. 2015; 362: 139–148. https://doi.org/10.1016/j.canlet.2015.03.036
[19] Greten FR, Eckmann L, Greten TF, Park JM, Li ZW, Egan LJ, et al. IKKbeta links inflammation and tumorigenesis in a mouse model of colitis-associated cancer. Cell. 2004; 118: 285–296. https://doi.org/10.1016/j.cell.2004.07.013
[20] Pikarsky E, Porat RM, Stein I, Abramovitch R, Amit S, Kasem S, et al. NF-kappaB functions as a tumour promoter in inflammation-associated cancer. Nature. 2004; 431: 461–466. https://doi.org/10.1038/nature02924
[21] Sovak MA, Bellas RE, Kim DW, Zanieski GJ, Rogers AE, Traish AM, et al. Aberrant nuclear factor-kappaB/Rel expression and the pathogenesis of breast cancer. The Journal of Clinical Investigation. 1997; 100: 2952–2960. https://doi.org/10.1172/JCI119848
[22] Baeuerle PA, Baltimore D. I kappa B: a specific inhibitor of the NF-kappa B transcription factor. Science (New York, N.Y.). 1988; 242: 540–546. https://doi.org/10.1126/science.3140380
[23] DiDonato JA, Hayakawa M, Rothwarf DM, Zandi E, Karin M. A cytokine-responsive IkappaB kinase that activates the transcription factor NF-kappaB. Nature. 1997; 388: 548–554. https://doi.org/10.1038/41493
[24] Zandi E, Rothwarf DM, Delhase M, Hayakawa M, Karin M. The IkappaB kinase complex (IKK) contains two kinase subunits, IKKalpha and IKKbeta, necessary for IkappaB phosphorylation and NF-kappaB activation. Cell. 1997; 91: 243–252. https://doi.org/10.1016/s0092-8674(00)80406-7
[25] Palombella VJ, Rando OJ, Goldberg AL, Maniatis T. The ubiquitin-proteasome pathway is required for processing the NF-kappa B1 precursor protein and the activation of NF-kappa B. Cell. 1994; 78: 773–785. https://doi.org/10.1016/s0092-8674(94)90482-0
[26] Sen R, Baltimore D. Multiple nuclear factors interact with the immunoglobulin enhancer sequences. Cell. 1986; 46: 705–716. https://doi.org/10.1016/0092-8674(86)90346-6
[27] Deregowski V, Delhalle S, Benoit V, Bours V, Merville MP. Identification of cytokine-induced nuclear factor-kappaB target genes in ovarian and breast cancer cells. Biochemical Pharmacology. 2002; 64: 873–881. https://doi.org/10.1016/s0006-2952(02)01151-6
[28] Jobin C, Hellerbrand C, Licato LL, Brenner DA, Sartor RB. Mediation by NF-kappa B of cytokine induced expression of intercellular adhesion molecule 1 (ICAM-1) in an intestinal epithelial cell line, a process blocked by proteasome inhibitors. Gut. 1998; 42: 779–787. https://doi.org/10.1136/gut.42.6.779
[29] Catz SD, Johnson JL. Transcriptional regulation of bcl-2 by nuclear factor kappa B and its significance in prostate cancer. Oncogene. 2001; 20: 7342–7351. https://doi.org/10.1038/sj.onc.1204926
[30] Guttridge DC, Albanese C, Reuther JY, Pestell RG, Baldwin AS, Jr. NF-kappaB controls cell growth and differentiation through transcriptional regulation of cyclin D1. Molecular and Cellular Biology. 1999; 19: 5785–5799. https://doi.org/10.1128/MCB.19.8.5785
[31] Namekawa T, Ikeda K, Horie-Inoue K, Suzuki T, Okamoto K, Ichikawa T, et al. ALDH1A1 in patient-derived bladder cancer spheroids activates retinoic acid signaling leading to TUBB3 overexpression and tumor progression. International Journal of Cancer. 2020; 146: 1099–1113. https://doi.org/10.1002/ijc.

32505
[32] Zito G, Naselli F, Saieva L, Raimondo S, Calabrese G, Guzzardo C, et al. Retinoic Acid affects Lung Adenocarcinoma growth by inducing differentiation via GATA6 activation and EGFR and Wnt inhibition. Scientific Reports. 2017; 7: 4770. https://doi.org/10.1038/s41598-017-05047-z
[33] Quintero Barceinas RS, García-Regalado A, Aréchaga-Ocampo E, Villegas-Sepúlveda N, González-De la Rosa CH. All-Trans Retinoic Acid Induces Proliferation, Survival, and Migration in A549 Lung Cancer Cells by Activating the ERK Signaling Pathway through a Transcription-Independent Mechanism. BioMed Research International. 2015; 2015: 404368. https://doi.org/10.1155/2015/404368
[34] Virmani AK, Rathi A, Zöchbauer-Müller S, Sacchi N, Fukuyama Y, Bryant D, et al. Promoter methylation and silencing of the retinoic acid receptor-beta gene in lung carcinomas. Journal of the National Cancer Institute. 2000; 92: 1303–1307. https://doi.org/10.1093/jnci/92.16.1303
[35] Kim DG, Choi EY, Ahn HM, Kim YJ. GRPR Drives Metastasis via CRABP2 and FNDC4 Pathways in Lung Adenocarcinoma. Cells. 2024; 13: 2128. https://doi.org/10.3390/cells13242128
[36] Facey COB, Hunsu VO, Zhang C, Osmond B, Opdenaker LM, Boman BM. *CYP26A1* Links WNT and Retinoic Acid Signaling: A Target to Differentiate ALDH+ Stem Cells in *APC*-Mutant CRC. Cancers. 2024; 16: 264. https://doi.org/10.3390/cancers16020264
[37] Lavudi K, Nuguri SM, Olverson Z, Dhanabalan AK, Patnaik S, Kokkanti RR. Targeting the retinoic acid signaling pathway as a modern precision therapy against cancers. Frontiers in Cell and Developmental Biology. 2023; 11: 1254612. https://doi.org/10.3389/fcell.2023.1254612
[38] Fu X, Zhang Q, Wang Z, Xu Y, Dong Q. CRABP2 affects chemotherapy resistance of ovarian cancer by regulating the expression of HIF1α. Cell Death & Disease. 2024; 15: 21. https://doi.org/10.1038/s41419-023-06398-4
[39] Chen Y, Tong X, Lu R, Zhang Z, Ma T. All-trans retinoic acid in hematologic disorders: not just acute promyelocytic leukemia. Frontiers in Pharmacology. 2024; 15: 1404092. https://doi.org/10.3389/fphar.2024.1404092
[40] Tobin RP, Cogswell DT, Cates VM, Davis DM, Borgers JSW, Van Gulick RJ, et al. Targeting MDSC Differentiation Using ATRA: A Phase I/II Clinical Trial Combining Pembrolizumab and All-Trans Retinoic Acid for Metastatic Melanoma. Clinical Cancer Research: an Official Journal of the American Association for Cancer Research. 2023; 29: 1209–1219. https://doi.org/10.1158/1078-0432.CCR-22-2495
[41] Lee SH, Shin JH, Shin MH, Kim YS, Chung KS, Song JH, et al. The Effects of Retinoic Acid and MAPK Inhibitors on Phosphorylation of Smad2/3 Induced by Transforming Growth Factor β1. Tuberculosis and Respiratory Diseases. 2019; 82: 42–52. https://doi.org/10.4046/trd.2017.0111
[42] Brown G. Deregulation of All-*Trans* Retinoic Acid Signaling and Development in Cancer. International Journal of Molecular Sciences. 2023; 24: 12089. https://doi.org/10.3390/ijms241512089
[43] Bahar ME, Kim HJ, Kim DR. Targeting the RAS/RAF/MAPK pathway for cancer therapy: from mechanism to clinical studies. Signal Transduction and Targeted Therapy. 2023; 8: 455. https://doi.org/10.1038/s41392-023-01705-z
[44] Sharma S, Shen T, Chitranshi N, Gupta V, Basavarajappa D, Sarkar S, et al. Retinoid X Receptor: Cellular and Biochemical Roles of Nuclear Receptor with a Focus on Neuropathological Involvement. Molecular Neurobiology. 2022; 59: 2027–2050. https://doi.org/10.1007/s12035-021-02709-y
[45] Doi A, Ishikawa K, Shibata N, Ito E, Fujimoto J, Yamamoto M, et al. Enhanced expression of retinoic acid receptor alpha (RARA) induces epithelial-to-mesenchymal transition and disruption of mammary acinar structures. Molecular Oncology. 2015; 9: 355–364. https://doi.org/10.1016/j.molonc.2014.09.005
[46] Chen C, Edelstein LC, Gélinas C. The Rel/NF-kappaB family directly activates expression of the apoptosis inhibitor Bcl-x(L). Molecular and Cellular Biology. 2000; 20: 2687–2695. https://doi.org/10.1128/MCB.20.8.2687-2695.2000
[47] Wu X, Sun L, Xu F. NF-κB in Cell Deaths, Therapeutic Resistance and Nanotherapy of Tumors: Recent Advances. Pharmaceuticals (Basel, Switzerland). 2023; 16: 783. https://doi.org/10.3390/ph16060783
[48] Zhang T, Ma C, Zhang Z, Zhang H, Hu H. NF-κB signaling in inflammation and cancer. MedComm. 2021; 2: 618–653. https://doi.org/10.1002/mco2.104
[49] Oh A, Pardo M, Rodriguez A, Yu C, Nguyen L, Liang O, et al. NF-κB signaling in neoplastic transition from epithelial to mesenchymal phenotype. Cell Communication and Signaling: CCS. 2023; 21: 291. https://doi.org/10.1186/s12964-023-01207-z
[50] Perucca P, Bassi E, Vetro M, Tricarico A, Prosperi E, Stivala LA, et al. Epithelial-to-mesenchymal transition and NF-kB pathways are promoted by a mutant form of DDB2, unable to bind PCNA, in UV-damaged human cells. BMC Cancer. 2024; 24: 616. https://doi.org/10.1186/s12885-024-12368-6
[51] Garg P, Jallepalli VR, Verma S. Unravelling the CXCL12/CXCR4 Axis in breast cancer: Insights into metastasis, microenvironment interactions, and therapeutic opportunities. Human Gene. 2024; 40: 201272. https://doi.org/10.1016/j.humgen.2024.201272
[52] Ebrahimi N, Abdulwahid AHRR, Mansouri A, Karimi N, Bostani RJ, Beiranvand S, et al. Targeting the NF-κB pathway as a potential regulator of immune checkpoints in cancer immunotherapy. Cellular and Molecular Life Sciences: CMLS. 2024; 81: 106. https://doi.org/10.1007/s00018-023-05098-8
[53] Xu Y, Yang L, Li G, Rao C. The Role of NF-κB/MIR155HG in Regulating the Stemness and Radioresistance in Breast Cancer Stem Cells. Frontiers in Bioscience (Landmark Edition). 2025; 30: 25810. https://doi.org/10.31083/FBL25810
[54] Zhang L, Ludden CM, Cullen AJ, Tew KD, Branco de Barros AL, Townsend DM. Nuclear factor kappa B expression in non-small cell lung cancer. Biomedicine & Pharmacotherapy = Biomedecine & Pharmacotherapie. 2023; 167: 115459. https://doi.org/10.1016/j.biopha.2023.115459
[55] Deen AJ, Adinolfi S, Härkönen J, Patinen T, Liu X, Laitinen T, et al. Oncogenic KEAP1 mutations activate TRAF2-NFκB signaling to prevent apoptosis in lung cancer cells. Redox Biology. 2024; 69: 103031. https://doi.org/10.1016/j.redox.2024.103031
[56] Gu L, Wang Z, Zuo J, Li H, Zha L. Prognostic significance of NF-κB expression in non-small cell lung cancer: A meta-analysis. PloS One. 2018; 13: e0198223. https://doi.org/10.1371/journal.pone.0198223
[57] Meylan E, Dooley AL, Feldser DM, Shen L, Turk E, Ouyang C, et al. Requirement for NF-kappaB signalling in a mouse model of lung adenocarcinoma. Nature. 2009; 462: 104–107. https://doi.org/10.1038/nature08462
[58] Zhou W, Chen X, Hu Q, Chen X, Chen Y, Huang L. Galectin-3 activates TLR4/NF-κB signaling to promote lung adenocarcinoma cell proliferation through activating lncRNA-NEAT1 expression. BMC Cancer. 2018; 18: 580. https://doi.org/10.1186/s12885-018-4461-z
[59] Chen Y, Zhu X, Wang J, Hu J, Zhang J, Zhang X, et al. MAZ promotes tumor proliferation and immune evasion in lung adenocarcinoma. Oncogene. 2024; 43: 3619–3632. https://doi.org/10.1038/s41388-024-03194-y
[60] Su Y, Amiri KI, Horton LW, Yu Y, Ayers GD, Koehler E, et al. A phase I trial of bortezomib with temozolomide in patients with

advanced melanoma: toxicities, antitumor effects, and modulation of therapeutic targets. Clinical Cancer Research: an Official Journal of the American Association for Cancer Research. 2010; 16: 348–357. https://doi.org/10.1158/1078-0432.CCR-09-2087

[61] Guo Q, Jin Y, Chen X, Ye X, Shen X, Lin M, et al. NF-κB in biology and targeted therapy: new insights and translational implications. Signal Transduction and Targeted Therapy. 2024; 9: 53. https://doi.org/10.1038/s41392-024-01757-9